^1H and ^{19}F NMR Study of Cation and Anion Motions in Guanidinium Fluoroantimonates

M. Grottel[a], A. Kozak[b], and Z. Pająk[b]

[a] Department of Physics, Academy of Agriculture, 60-637 Poznań, Poland
[b] Institute of Physics, A. Mickiewicz University, 61-614 Poznań, Poland

Z. Naturforsch. **50a**, 742–748 (1995); received March 2, 1995

Proton and fluorine NMR linewidths, second moments, and spin-lattice relaxation times of polycrystalline $[C(NH_2)_3]_2SbF_5$ and $C(NH_2)_3SbF_6$ were studied in a wide temperature range. For the pentafluoroantimonate, C_3-reorientation of the guanidinium cation and C_4-reorientation of the SbF_5 anion were revealed and their activation parameters determined. The dynamical inequivalence of the two guanidinium cations was evidenced. For the hexafluoroantimonate, two solid-solid phase transitions were found. In the low temperature phase the guanidinium cation undergoes C_3 reorientation while the SbF_6 anion reorients isotropically. The respective activation parameters were derived. At high temperatures new ionic plastic phases were evidenced.

Key words: NMR, Molecular Motions, Phase transitions

Introduction

Extensive NMR studies of the molecular dynamics in guanidinium salts have been performed in our laboratory [1–8]. In all the compounds reorientation of the guanidinium cation around its C_3 symmetry axis, accompanied by a motion of NH_2 groups was evidenced. In salts containing fluorine in their anions the dynamics of both ions was described. For guanidinium tetrafluoroborate [3], hexafluorophosphate [4], hexafluoroaluminate [5] and gallate [6] we found isotropic reorientation of the anions. The study of ^1H and ^{19}F NMR second moments and relaxation times as well as an analysis of all cross-relaxation interactions allowed us to derive the Arrhenius activation parameters for the motions considered. Later a convergence of the rotational correlation times of cation and anion at the phase transition was revealed. This effect points to a coupling of rotational modes which may drive the respective phase transition. The present work deals with bis-guanidinium pentafluoroantimonate $[C(NH_2)_3]_2SbF_5$ (GPFA) and guanidinium hexafluoroantimonate $[C(NH_2)_3]_2SbF_6$ (GHFA), compounds suitable for a study of both ionic sublattices.

GPFA crystallizes in a C2/m space group with $a=15.900$ (4), $b=8.456$ (2), $c=9.725$ (3) Å, $\beta=121.19°$ (2), $V=1118.5$ (5) Å^3 and $Z=4$ [9]. The crystal structure consists of two sets of guanidinium sheets linked by rather strong N–H...F hydrogen bonds to pentafluoroantimonate ions. The two inequivalent guanidinium ions Gu1 and Gu2 are planar, while the SbF_5 anion is a square pyramid with the axial fluorine atom acting as the weakest hydrogen bond acceptor. It was interesting to check whether the structural inequivalence of cations influences their motional behaviour seen in the NMR experiments.

The crystal structure of GHFA has not been determined, but the compound seems to be worth studying because of the solid-solid phase transitions we have discovered. It was interesting to see whether the effect of coupling of rotational modes of the cation and anion sublattices can be evidenced for this compound as well.

To examine the dynamics of cations and anions in both salts, a proton and fluorine NMR study of second moments, line shapes and spin-lattice relaxation times, complemented by differential thermal analysis, has been undertaken in a wide range of temperature.

Experimental

GPFA and GHFA were obtained by the reactions

$$[C(NH_2)_3]_2CO_3 + 2HF + SbF_3 \Rightarrow [C(NH_2)_3]_2SbF_5 + CO_2 + H_2O,$$

$$[C(NH_2)_3]_2CO_3 + Sb_2O_5 + 12HF \Rightarrow 2C(NH_2)_3SbF_6 + CO_2 + 6H_2O.$$

Reprint requests to Prof. Z. Pająk.

0932-0784 / 95 / 0800-0742 $ 06.00 © – Verlag der Zeitschrift für Naturforschung, D-72027 Tübingen

The products, recrystallized from 90% ethanol, were ground to a powder, degassed and sealed under vacuum in glass ampoules.

The measurements of proton and fluorine NMR second moments were carried out with a wide-line spectrometer operating at 28.0 and 26.3 MHz for protons and fluorines, respectively. The second moments were calculated by numerical integration of the first derivative of an absorption line and corrected for finite modulation amplitude. Mean values were obtained for about 10 derivatives registered at each temperature.

The measurements of proton and fluorine spin-lattice relaxation times T_1 were performed with a 60 MHz pulse NMR spectrometer by a saturation recovery method. The fluorine relaxation time $T_{1\varrho}$ was measured at 25 MHz in a rotating field of 18 G by a spin-locking method in the temperature range 185–320 K. The temperature of the sample was controlled to an accuracy of 1 K.

Differential thermal analysis (DTA) was made with a Derivatograph Unipan (DSC 605MD).

Results

The temperature dependence of the proton second moment and linewidth for GPFA is shown in Figure 1. The proton second moment of about 23 G^2 observed below 250 K decreases to 4.2 G^2 achieved above 420 K. The proton linewidth starts to decrease at about 330 K from 12.6 G to 4.2 G. The temperature dependence of the fluorine second moment and linewidth for GPFA is shown in Figure 2. The fluorine second moment decreases from 13.5 G^2 at about 250 K to 2 G^2 above 370 K. The fluorine linewidth decreases at about 250 K from 8.5 G to 2.8 G.

Figures 3 and 4 show the temperature dependences of the proton and fluorine second moments and the linewidths for GHFA. The proton second moment of 23.3 G^2 observed at low temperatures decreases to 4 G^2 above 330 K, and at 410 K starts to fall to a negligible value determined by the magnetic field inhomogeneity. Similarly, the fluorine second moment decreases from 10.5 G^2 to 1.4 G^2 above 330 K and at 410 K falls to 0.4 G^2. The proton and fluorine linewidths reflect the changes of the second moments observed. Figure 5 shows the shapes of the proton and fluorine NMR line derivatives registered for GHFA at three different temperatures.

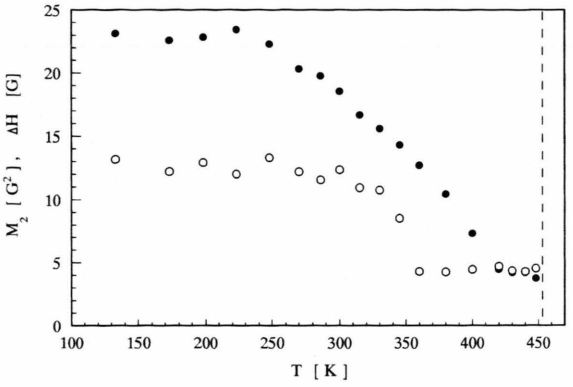

Fig. 1. Temperature dependences of the proton second moment M_2 (●) and linewidth ΔH (○) for GPFA.

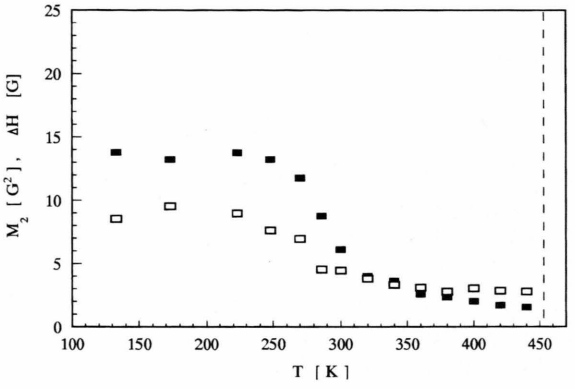

Fig. 2. The temperature dependences of the fluorine second moment M_2 (■) and linewidth ΔH (□) for GPFA.

The temperature dependences of the proton and fluorine spin-lattice relaxation times for GPFA and GHFA are shown as log T_1 against inverse temperature in Figs. 6 and 7, respectively. For both compounds in the whole temperature range a nonexponential magnetization recovery is observed for protons and fluorines. The decay curves were decomposed into two exponential terms with different T_1 values. For clarity only the main T_1 components for magnetization amplitudes higher than 0.5 are shown in the figures. For GPFA one can see the diminishing of the proton T_1 with increasing temperature and the minimum of the fluorine T_1 of 18 ms at about 390 K. More complicated T_1 temperature dependences have been obtained for GHFA (Figure 7). Figure 8 shows the temperature variation of the relaxation time $T_{1\varrho}$ for GPFA, revealing a minimum of 0.7 ms at about 300 K.

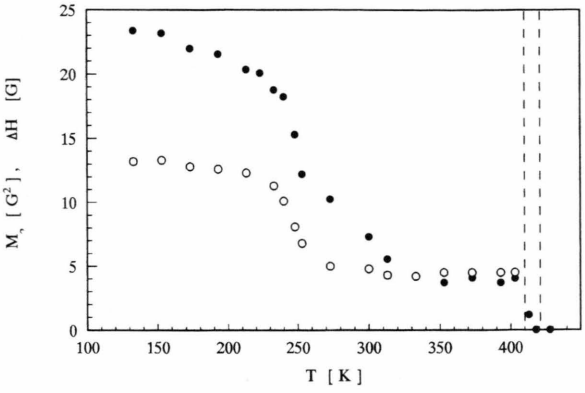

Fig. 3. Temperature dependences of the proton second moment M_2 (●) and linewidth ΔH (○) for GHFA.

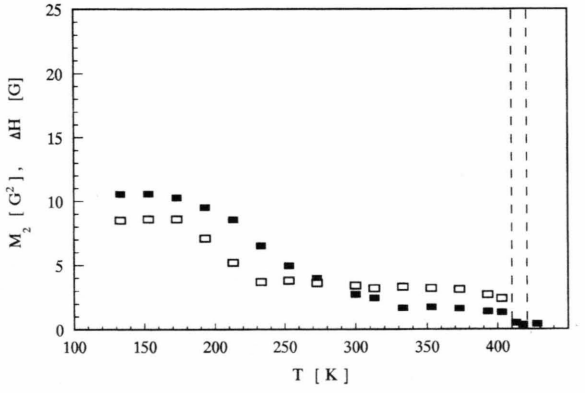

Fig. 4. Temperature dependences of the fluorine second moment M_2 (■) and linewidth ΔH (□) for GHFA.

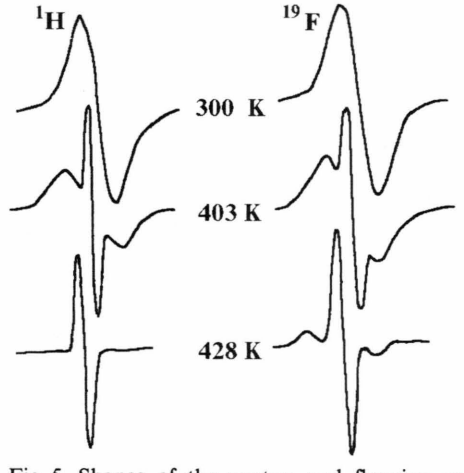

Fig. 5. Shapes of the proton and fluorine resonance line derivatives for GHFA registered at three different temperatures.

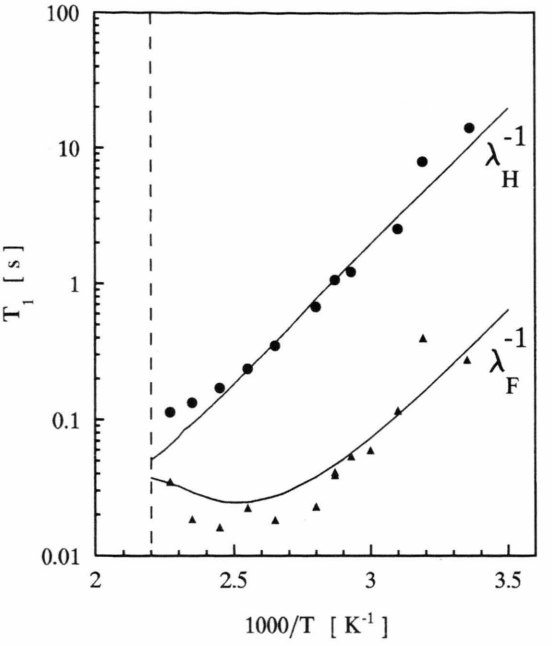

Fig. 6. Temperature dependence of the proton (●) and fluorine (▲) spin-lattice relaxation time T_1 for GPFA. The full curves are theoretical fits.

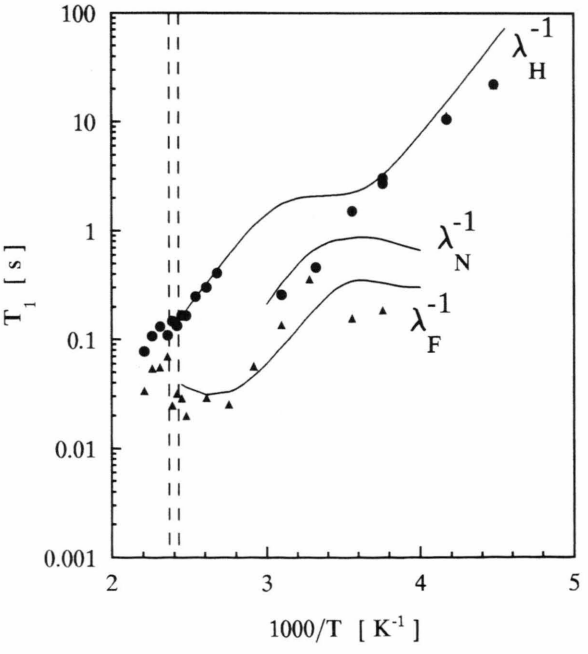

Fig. 7. Temperature dependence of the proton (●) and fluorine (▲) spin-lattice relaxation time T_1 for GHFA. The full curves are theoretical fits.

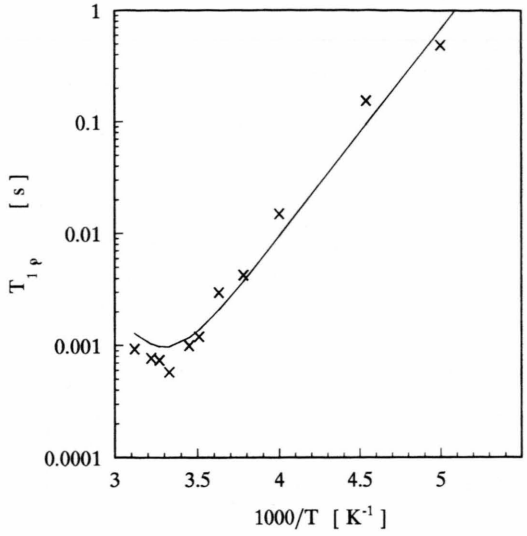

Fig. 8. Temperature dependence of the fluorine rotating frame relaxation time $T_{1\varrho}$ for GPFA. The full curve is the theoretical fit.

A DTA study for GPFA has confirmed the melting point at 453 K reported earlier [10]. For GHFA two specific heat anomalies were observed at 410 and 421 K. Thermal gravimetry analysis suggests the decomposition of the compound above 500 K.

Calculations and Discussion

Guanidinium Pentafluoroantimonate

The theoretical proton and fluorine Van Vleck [11] second moment values for the rigid structure of the compound were found numerically using our X-ray data [9]. Contributions from all kinds of magnetic nuclei occurring in the sample were taken into account. Table 1 presents the proton M_2^H and fluorine M_2^F second moments values thus obtained.

As one can see, the structural inequivalence of the two guanidinium cations (Gu1 and Gu2) is not reflected in the calculated values of their rigid lattice second moments. The mean value 23.95 G^2 agrees well with the experimental $M_2^H = 23$ G^2 registered at the low temperatures.

Similarly, for fluorines, a very good agreement between the theoretical ($M_2^F = 13.4$ G^2) and experimental ($M_2^F = 13.5$ G^2) values at low temperatures was obtained. This means that at those temperatures both ion sublattices are rigid on the NMR time scale.

Table 1. Second moments calculated for the rigid structure of $[C(NH_2)_3]_2SbF_5$.

Interaction	M_2^H [G^2]		Interaction	M_2^F [G^2]
	Gu1	Gu2		
H–H	18.57	18.53	F–F	3.25
H–N	2.05	1.98	F–Sb	1.18
H–F	3.32	3.28	F–H	8.96
H–Sb	0.07	0.10	F–N	0.00
Total	24.01	23.89	Total	13.39

On increase in temperature the second moments are evidently reduced, reflecting the onset of ion motions in the crystal lattice. The observed reduction of the proton second moment ($\Delta M_2^H \approx 19$ G^2) can be explained in terms of the guanidinium cations reorientation around their C_3 symmetry axes accompanied by an NH_2 groups motion. A similar model of the guanidinium reorientation was reported for a number of guanidinium salts [1–8].

Though the calculated values of the proton rigid lattice second moments for the two crystallographically inequivalent guanidinium cations do not differ, the temperature variation of the proton lineshape and linewidth as well as the broad temperature region in which the second moment diminishes suggest that the two guanidinium cations differ in their motional freedom. Up to about 400 K the NMR line consists of two components, corresponding to two different cations. The linewidth plot reveals the temperature behaviour of the broader component, ascribed to the less mobile cation. The activation energies estimated roughly from the Waugh-Fiedin formula [12] for the two dynamically inequivalent guanidinium cations are 38 and 50 kJ/mol.

For the fluorines, the M_2^F value of 2 G^2 observed at high temperatures agrees very well with the values calculated for the SbF_5 anion reorientation around its C_4 symmetry axis (1.9 G^2). The apparent activation energy estimated from the fluorine second moment plot amounts to 38 kJ/mol. The same value is found for one of the guanidinium cations. However, our M_2 experiment does not decide whether the cation or anion starts to reorient first, because of significant modulation of proton-fluorine and/or fluorine-proton interactions resulting from the onset the ionic reorientations. Thus the spin-lattice relaxation experiment was expected to reveal more conclusive details concerning the ions motions. Different dynamic models

were considered, and adequate reduced second moments ΔM_2^H and ΔM_2^F have been used to calculate diagonal and off-diagonal relaxation matrix elements R_{II} and R_{IS}:

$$R_{II} = \frac{2}{3}\gamma_I^2 \Delta M_2^{II} g_1(\omega_I, \tau) + \frac{1}{2}\sum_S \gamma_I^2 \Delta M_2^{IS} g_2(\omega_I, \omega_S, \tau),$$

$$R_{IS} = \frac{1}{2}\gamma_S^2 \Delta M_2^{SI} g_3(\omega_I, \omega_S, \tau) N_S/N_I,$$

where

$$g_1(\omega_I, \tau) = \tau/(1 + \omega_I^2\tau^2) + 4\tau/(1 + 4\omega_I^2\tau^2),$$
$$g_2(\omega_I, \omega_S, \tau) = \tau/[1 + (\omega_I - \omega_S)^2\tau^2] + 3\tau/(1 + \omega_I^2\tau^2) + 6\tau/[1 + (\omega_I + \omega_S)^2\tau^2],$$
$$g_3(\omega_I, \omega_S, \tau) = -\tau/[1 + (\omega_I - \omega_S)^2\tau^2] + 6\tau/[1 + (\omega_I + \omega_S)^2\tau^2].$$

Since the compound studied is a multispin system, we considered the relaxation matrix for four – spins (H, F, Sb^{121}, Sb^{129}) and applied our procedure described in [4]. The dipolar interactions with N^{14} nuclei were taken into account in the calculations of the diagonal R_{HH} element of the relaxation matrix. All quadrupolar interactions could be neglected because of fast ionic reorientations.

The inverses of the calculated proton and fluorine eigenvalues λ_H and λ_F for the relaxation matrix were fitted to the T_1 experimental data. The calculations have involved three adjustable parameters for each dynamical process: the activation energy E_a, the pre-exponential factor τ_0 for assumed Arrhenius behaviour, and the value of proton–fluorine or fluorine–proton interaction (ΔM_2^{H-F} or ΔM_2^{F-H}).

A reasonable fit to the experimental data was obtained for the model assuming C_4 reorientation of the SbF_5 anion followed by reorientations of guanidinium cations overcoming different potential barriers. The respective activations parameters are listed in Table 2.

Our temperature study of the fluorine rotating – frame relaxation time $T_{1\varrho}$ confirms the model of the anion reorientation considered. Taking into account only the fluorine – fluorine interaction, the experimental $T_{1\varrho}$ data could be described by the expression

$$T_{1\varrho}^{-1} = C_{FF} \cdot g_\varrho(\omega_0, \omega_1, \tau),$$

where

$$g_\varrho(\omega_0, \omega_1, \tau) = \frac{5}{2}\frac{\tau}{1 + \omega_0^2\tau^2} + \frac{\tau}{1 + 4\omega_0^2\tau^2} + \frac{3}{2}\frac{\tau}{1 + 4\omega_1^2\tau^2}$$

and

$$C_{FF} = \frac{2}{3}\gamma_F^2 \Delta M_2^{FF}.$$

Using the activation parameters for the anion motion derived from the T_1 experiment (Table 2) a satisfactory agreement between theoretical and experimental data has been obtained (Figure 8).

The activation energies for the C_3 reorientation of both guanidinium cations are markedly different, reflecting different networks of hydrogen bonds in which both cations are involved. The values obtained are comparable with those characterizing the motion of the cation embedded in similar anion sublattices [3–8]. Unlike the *isotropic* motion of the fluorinated anions PF_6, AlF_6, GaF_6 and BF_4, the SbF_5 anion has been found to undergo the *anisotropic* C_4 reorientation. This type of motion was reported in other salts containing the SbF_5 square pyramidal anions [10, 13, 14].

Table 2. The activation parameters of $[C(NH_2)_3]_2SbF_5$.

Ion	E_a [kJ/mol]	τ_0 [s]
Gu1–C_3	41.9	$6.3 \cdot 10^{-14}$
Gu2–C_3	52.8	$6.9 \cdot 10^{-15}$
SbF_5	34.8	$2.2 \cdot 10^{-13}$

Guanidinium Hexafluoroantimonate

Despite the unknown crystal structure of the compound, the proton second moment of 23.3 G^2 registered at the lowest temperatures can be considered as corresponding to the rigid cation sublattice since a similar value was found for GPFA and other guanidinium salts.

For the calculation of the fluorine second moment we assume the Sb–F distance to be 1.87 Å, as often reported [15]. Hence, estimating $M_2^{F-F} = 5\ G^2$, $M_2^{F-Sb} = 2\ G^2$ and $M_2^{F-H} = 3.9\ G^2$ (the latter derived from the M_2^{H-F} value) one obtains a total second moment of 10.9 G^2 for the rigid lattice structure of the anions, in good agreement with the experiment at low temperatures.

The reduction of the proton second moment from 23.3 to 4 G^2, similar to that observed in GPFA, can also be interpreted as resulting from the C_3 reorienta-

tion of the guanidinium cation and NH_2 group motion. This state of motion is preserved up to the first phase transition at 410 K, above which the second moment drops almost to zero, pointing to the onset of cationic self-diffusion. The line shape analysis (Fig. 5) shows that the slow diffusive process starts already at about 330 K, where a narrow line appears growing in intensity with temperature. Above the phase transition at 410 K the broad line disappears and only a liquid-like NMR line is observed.

The reduction of the fluorine second moment from 10.5 G^2 to 1.4 G^2 can be interpreted as resulting from the isotropic reorientation of the hexafluoroantimonate anions. Above 330 K the fine structure of the fluorine spectrum is similar to that for protons (Figure 5). The intensity of the appearing narrow line increases with temperature. However, above the first phase transition at 410 K, contrary to protons, the broad component is still observed and does not disappear even above the second phase transition at 421 K. The narrow liquid-like component of the spectrum points to the existence of anionic self-diffusion appearing beside the evidenced isotropic reorientation of the anions.

Spin-lattice relaxation experiments allow to derive the activation parameters for the reorientation of the cation and anion. To interpret the experimental T_1 data we considered, similarly as for GPFA, the relaxation matrix for four spins and applied the same procedure as described in [4]. The analysis performed has shown the model of motions to be consistent with that resulting from the second moment experiment, that is: C_3 reorientation of the guanidinium cation accompanied by NH_2 group motion and isotropic reorientation of the anion. The activation energy for the reorientations of the cation is similar to values reported for other guanidinium salts [3–8]. The activation parameters derived from the fitting procedure are presented in (Table 3).

Table 3. The activation parameters of $[C(NH_2)_3SbF_6$.

Ion	E_a [kJ/mol]	τ_0 [s]
Gu–C_3	41.5	$8.0 \cdot 10^{-14}$
Gu–NH_2	23.0	$4.0 \cdot 10^{-14}$
SbF_6	33.9	$5.3 \cdot 10^{-13}$

It is interesting to note that in the high temperature phases the cation motion is described by simultaneous isotropic reorientation and self diffusion reducing all intra- and interionic interactions to zero. Such a behaviour, which has previously been found in guanidinium perchlorate [1] and hexachloroantimonate [8], characterises ionic plastic phases. For the fluorine sublattice one observes a coexistence of liquid-like and solid-like anions. Thus the plastic character of this sublattice seems to be less pronounced probably due to a slower diffusion process.

The activation parameters obtained for the motions considered allowed to determine the temperature dependences of the proton and fluorine correlation times τ^H and τ^F characterizing stochastic reorientations of the ions. For both compounds one observes that rotational correlation times for the cation and anion tend to converge at respective phase transitions, similarly as was found earlier in a number of other salts [16–19].

Conclusions

1. In GPFA dynamical inequivalence of the two crystallographically inequivalent guanidinium cations was evidenced. Both cations undergo C_3 reorientations overcoming different potential barriers. An anisotropic C_4 reorientation of the anion has been revealed.

2. In GHFA two solid-solid phase transitions were found. In the low temperature phase the guanidinium cation undergoes C_3 reorientation, while the anion reorients isotropically around its center of gravity. The motional behavior of both ions changes dramatically at the highest temperatures, revealing the existence of ionic plastic phases.

3. In both compounds a convergence of the reorientational correlation times of the cation and anion has been observed within the accuracy limits at the respective phase transitions.

Acknowledgements

The present work has been supported by the Committee for Scientific Research under Grant No. 2 P03B 065 08.

[1] Z. Pająk, M. Grottel, and A. Kozioł, J. Chem. Soc., Faraday Trans. 2, **78,** 1529 (1982).
[2] M. Grottel and Z. Pająk, J. Chem. Soc., Faraday Trans. 2, **80,** 553 (1984).
[3] A. Kozak, M. Grottel, A. Kozioł, and Z. Pająk, J. Phys. C, Solid State Phys. **20,** 5433 (1987).
[4] M. Grottel, A. Kozak, A. Kozioł, and Z. Pająk, J. Phys.: Condens. Matter **1,** 7069 (1989).
[5] M. Grottel, A. Kozak, H. Małuszyńska, and Z. Pająk, J. Phys.: Condens. Matter 4, 1837 (1992).
[6] A. Kozak, M. Grottel, and Z. Pająk, Acta Phys. Polonica, **83,** 219 (1993)
[7] J. Wąsicki, M. Grottel, A. Kozak, and Z. Pająk, J. Phys.: Condens. Matter **6,** 2491 (1994).
[8] Z. Pająk, and J. Zaleski, Solid State Commun. **91,** 821 (1994).
[9] H. Małuszyńska, Acta Cryst. **C50,** 1909 (1994).
[10] I. Moskvich, A. Polyakov, B. Cherkasov, A. Sukhovski, and L. Davidovich, Raport no 504, Akademia Nauk SSSR Krasnoyarsk (1988).
[11] J. H. Van Vleck, Phys. Rev. **74,** 1168 (1948).
[12] J. S. Waugh and E. I. Fiedin, Fiz. Tverd. Tela, **4,** 2233 (1962).
[13] S. Miyajima, N. Nakamura, and H. Chihara, J. Phys. Soc. Japan **49,** 1867 (1980).
[14] V. I. Sergenko, V. J. Kavun, and L. H. Ignateva, Zhurn. Neorg. Khim. **12,** 3153 (1991).
[15] R. F. Copeland, S. H. Conner, and E. A. Meyers, J. Phys. Chem. **70,** 1288 (1968).
[16] Z. Pająk, A. Kozak, and M. Grottel, Solid. State Commun. **65,** 671 (1988).
[17] A. Kozak, M. Grottel, J. Wąsicki, and Z. Pająk, Phys. Stat. Sol. (a) **141,** 345 (1994).
[18] M. Grottel, A. Kozak, J. Wąsicki, and Z. Pająk, Proc. XXV Sem. NMR Cracow 1987 p 208.
[19] Z. Pająk, Solid State Commun. **92,** 707 (1994).